

THE SOLAR X-RAY CONTINUUM MEASURED BY RESIK

K. J. H. Phillips¹

Mullard Space Science Laboratory, University College London, Holmbury St Mary,
Dorking, Surrey RH5 6NT, U.K.

`kjhp@mssl.ucl.ac.uk`

and

J. Sylwester and B. Sylwester²

Space Research Centre, Polish Academy of Sciences, 51-622, Kopernika 11, Wrocław,
Poland

`js@cbk.pan.wroc.pl`, `bs@cbk.pan.wroc.pl`

and

V. D. Kuznetsov³

Institute of Terrestrial Magnetism and Radiowave Propagation (IZMIRAN), Troitsk,
Moscow, Russia

`kvd@izmiran.ru`

Received _____; accepted _____

To be published, Astrophysical Journal

ABSTRACT

The solar X-ray continuum emission at five wavelengths between 3.495 Å and 4.220 Å for 19 flares in a seven-month period in 2002–2003 was observed by the RESIK crystal spectrometer on *CORONAS-F*. In this wavelength region, free–free and free–bound emissions have comparable fluxes. With a pulse-height analyzer having settings close to optimal, the fluorescence background was removed so that RESIK measured true solar continuum in these bands with an uncertainty in the absolute calibration of $\pm 20\%$. With an isothermal assumption, and temperature and emission measure derived from the ratio of the two *GOES* channels, the observed continuum emission normalized to an emission measure of 10^{48} cm^{-3} was compared with theoretical continua using the CHIANTI atomic code. The accuracy of the RESIK measurements allows photospheric and coronal abundance sets, important for the free–bound continuum, to be discriminated. It is found that there is agreement to about 25% of the measured continua with those calculated from CHIANTI assuming coronal abundances in which Mg, Si, Fe abundances are four times photospheric.

Subject headings: Sun: abundances — Sun: corona — Sun: flares — Sun: X-rays, gamma rays

1. INTRODUCTION

The RESIK (REntgenovsky Spektrometr s Izognutymi Kristalami) X-ray spectrometer on the *CORONAS-F* solar spacecraft obtained numerous solar X-ray spectra in the range 3.40–6.05 Å from shortly after the spacecraft launch (on 2001 July 31) to 2003 May. The instrument (Sylwester et al. 2005) was a bent crystal spectrometer with four channels, the solar X-ray emission being diffracted by silicon and quartz crystals. Pulse-height analyzers enabled solar photons to be distinguished from those produced by fluorescence of the crystal material (photon energies of $\gtrsim 1.84$ keV, the K-shell ionization energy of Si) through the different energies of the photons. This has meant that the instrumental background, which has been a significant problem for most previous spacecraft crystal spectrometers (e.g. Culhane et al. (1991)), could be eliminated for channels 1 and 2 (Si 111 crystal, $2d = 6.27$ Å) since for these channels the range of solar photon energies are substantially different (3.26–3.64 keV and 2.90–3.24 keV). For channels 3 and 4 (quartz 10 $\bar{1}$ 0 crystal, $2d = 8.51$ Å), the photon energies are closer and the discrimination is only partial, but the fluorescence can nevertheless be accurately estimated. Thus, a means of measuring the solar continuum is offered. The spectral ranges of RESIK for on-axis solar sources are: channel 1, 3.40–3.80 Å; channel 2, 3.83–4.27 Å; channel 3, 4.35–4.86 Å; and channel 4, 5.00–6.05 Å. RESIK was uncollimated to maximize the instrument’s sensitivity; this leads to some degree of spectral confusion only on the rare occasions when two simultaneous flares occurred on the Sun. While previous work on RESIK spectra has concentrated on line spectra (Sylwester et al. 2006; Phillips et al. 2006a; Chifor et al. 2007; Sylwester et al. 2008, 2009), here we discuss continuum emission observed during flares. There are several portions of the X-ray spectrum observed by RESIK in channels 1 and 2 that are practically free of lines and therefore enable the X-ray continuum flux to be estimated. Few such observations have provided accurate continuum fluxes in this wavelength region.

With estimates of temperature T_{GOES} and emission measure of the emitting regions available from the flux ratio of the two channels of *GOES*, we have been able to examine the continuum emission at available wavelengths as a function of T_{GOES} . We have compared this with calculated continua from the CHIANTI atomic database and code (Landi et al. 2006). The wavelength range concerned (3.5–4.2 Å) is of particular interest because within it free–bound emission is comparable to free–free emission, so the accuracy of particularly the free–bound emission calculations can be verified. The free–bound emission depends on the set of abundances used in the calculations, a coronal set (Feldman (1992); Fludra & Schmelz (1999)) giving rise to greater emission than a photospheric set (Grevesse et al. 2007; Asplund et al. 2009). The accuracy of the photometric calibration of RESIK is such that this difference can be detected. Further, recent calculations (Brown et al. 2009) suggest that free–bound emission may sometimes significantly contribute to the total non-thermal continuum during solar flare impulsive stages and so a check on the thermal continuum at high temperatures as calculated by CHIANTI and other codes is very desirable.

2. THEORETICAL CONTINUA

We first describe calculations using CHIANTI of free–free, free–bound, and two-photon continua emitted by a solar coronal plasma. These were obtained from functions available in the IDL-based SolarSoft system (Freeland & Handy 1998). The CHIANTI free–free continua are based on fitting formulas given by Sutherland (1998) and Itoh et al. (2000). Ionization fractions which are needed as input to both free–free and free–bound continua were from the recent work of Bryans et al. (2009). Element abundances also affect the free–bound continuum. It is found that the continua in the RESIK wavelength range are made up of free–free and free–bound continua in comparable amounts. For the temperatures

and wavelengths considered here, two-photon continua (arising from the de-excitation of metastable levels in H-like and He-like ions) are a factor ~ 30 less than either free-bound or free-free continuum emission, and were therefore neglected.

For the wavelengths considered here (3.40–4.27 Å), free-bound emission is especially important for coronal abundances at flare-like temperatures ($\lesssim 20$ MK). Large contributions to the total emission are made by recombination to Si, Fe, and Mg ions, and to some extent O ions. The coronal abundances of Si, Fe, and Mg are higher than the corresponding photospheric abundances according to the “FIP” effect, for which elements with first ionization potential (FIP) lower than 10 eV have enhanced coronal abundances. The free-bound emission is thus greater for coronal abundances by amounts that depend on the exact abundance set assumed. In this work, we took coronal abundances from Feldman (1992) and Fludra & Schmelz (1999), and photospheric abundances from Grevesse et al. (2007). (The coronal abundances of Feldman & Laming (2000) are similar to those of Feldman (1992) for C, N, O, Ne, and Ar, but similar to those of Fludra & Schmelz (1999) for Mg, Si, S, Ca, and Fe; the photospheric abundances of Asplund et al. (2009) are within 20% of those of Grevesse et al. (2007) except for Ar for which Asplund et al. (2009) is 65% larger.) Edge features in the continuum are formed when free electrons recombine with fully stripped and H-like Si ions at 5.08 Å and 4.64 Å (2.44 keV, 2.67 keV); with fully stripped and H-like Mg ions at 7.05 Å, 6.33 Å (1.76 keV, 1.96 keV); and with fully stripped and H-like S ions at 3.55 Å, 3.85 Å (3.49 keV, 3.22 keV). Recombination of electrons with a range of Fe ions gives rise to edges between 6 Å and 9.1 Å (1.36–2.1 keV). There are upward jumps in the free-bound emission below each of these wavelengths. This gives rise to an accumulation of emission at wavelengths $\lesssim 9$ Å for a large temperature range. The S edges fall within the range considered here and so may be important. To the free-bound emission must be added free-free continuum, due mostly to H and He, with very small contributions from heavier elements.

Figure 1 (*left panel*) shows the total free–free, free–bound continuum emission from CHIANTI and their sum in the 1–11 Å range (which therefore includes the range of all RESIK detectors) for electron temperature $T_e = 15$ MK and the Feldman (1992) coronal abundance set. A volume emission measure of 10^{48} cm $^{-3}$ is assumed. For other temperatures, the relative continuum fluxes are quite similar. Individual contributions made by O, Si, Mg, S, and Fe ions to the free–bound emission are indicated by the different line symbols: it can be seen how large these contributions are at various wavelengths. For the 3.5–4.2 Å range, the contributions to the total free–bound continuum made by Fe and Si are each 31%, Mg 18%, and O 13%. The use of coronal or photospheric abundances for these elements is clearly a matter of some importance. According to Feldman (1992), the coronal abundances are greater than those of Grevesse et al. (2007) by factors of 1.7 (O), 4 (Mg and Si), and 4.5 (Fe). The corresponding factors for the coronal abundance set of Fludra & Schmelz (1999) are 1.2 (O) and between 2.3 and 2.4 for Mg, Si, and Fe. For S, the coronal abundances are only slightly higher (between 17% and 34%) than photospheric abundances. Figure 1 (*right panel*) shows the differences for coronal (Feldman 1992) and photospheric (Grevesse et al. 2007) abundance sets. At 4.0 Å the free–bound continuum is a factor > 2 higher for coronal abundances, and the total continuum is higher by 70%. (The free–free continuum is only $\sim 10\%$ lower for the photospheric abundances of Grevesse et al. (2007).) This is larger than the expected uncertainties (20%) in the RESIK absolute flux calibration, offering the possibility of distinguishing element abundance sets through RESIK observations of the continuum emission.

A further illustration of the effect of abundances is given in Figure 2: in this case, continuum fluxes at 3.495 Å are plotted against T_e for coronal (Feldman (1992): left panel) abundances and photospheric (Grevesse et al. (2007): center panel) abundances and their ratios (right panel). Again, an emission measure of 10^{48} cm $^{-3}$ is assumed. There are differences of a factor 2–3 in the free–bound continua, though at longer wavelengths the

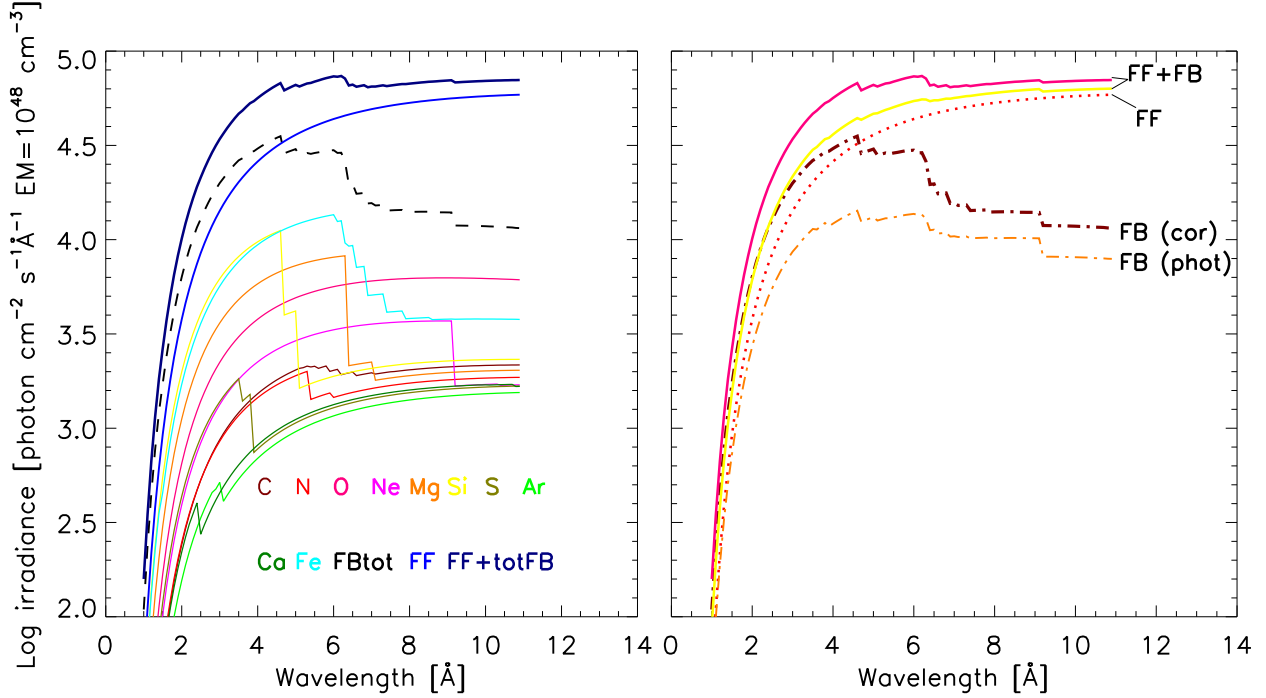


Fig. 1.— *Left panel:* Continuum fluxes (irradiance, photon units) calculated from the CHIANTI atomic package at $T_e = 15$ MK and an emission measure 10^{48} cm^{-3} plotted against wavelength (1–11 Å). The solid line shows the sum of free–free (FF) and free–bound (FB) continua, the dotted lines the free–free and free–bound continua for all elements. Other curves show the contributions to the free–bound continua made by individual elements (O, Fe, Si, Mg, S) with coronal abundances (Feldman (1992)). *Right panel:* Continuum fluxes compared for coronal (Feldman (1992)) and photospheric (Grevesse et al. (2007)) abundances for $T_e = 15$ MK. Solid lines are the total of free–free and free–bound, the dot–dash curves are for free–bound (FB), coronal and photospheric abundances indicated. The dotted curve is the free–free continuum for coronal abundances (free–free emission for photospheric abundances is about 10% lower). [A color version of this figure is available in the on-line version of the journal, showing free–bound emission from more elements: color key is C (maroon); N (red); O (pink); Ne (magenta); Mg (orange); Si (yellow); S (olive); Ar (green); Ca (dark green); Fe (cyan); free–free emission (blue); and total emission (dark blue).]

differences are less. For 3.495 Å, free-bound emission is equal to free-free at a temperature of 17 MK for coronal abundances, but a much smaller temperature (9 MK) for photospheric abundances.

X-ray continua from the analytical formulae of Culhane & Acton (1970) and Gronenschild & Mewe (1978), calculated on the basis of coronal abundances adopted by these authors, have been widely used in the past. These abundances are different from the more definitive work of Feldman (1992), and partly as a result of this, there are differences of up to 60% from the CHIANTI curves with the Feldman (1992) coronal abundances for the wavelengths considered here. The wavelength dependence of the total emission is, however, very similar in all three cases.

3. OBSERVATIONS AND ANALYSIS

A sample of 19 flares, all with few or no interruptions in the time coverage, was selected from the RESIK data base. A total of 2795 spectra was analyzed. Table 1 gives a list of time periods during flares when RESIK observations were taken and analyzed.¹ The *GOES* class, peak times, and heliographic coordinates of the host active region are given. The spectra were accumulated in data-gathering time intervals (DGIs) that were automatically adjusted using on-board software according to the incident X-ray flux. During large flares of *GOES* class equal to at least M1, the DGI typically decreased from a few minutes at the flare onset to only ~ 2 s at flare peak, then increased again during the flare decline. The pulse-height analyzers on RESIK (by which solar X-ray photons are distinguished from crystal fluorescence photons) had settings that were varied over the first few months of the spacecraft mission and spectra examined to find the optimum settings; the flare spectra analyzed in this study were taken when the settings were established to be close to optimum. The spectra in channels 1 and 2 were converted to absolute flux units

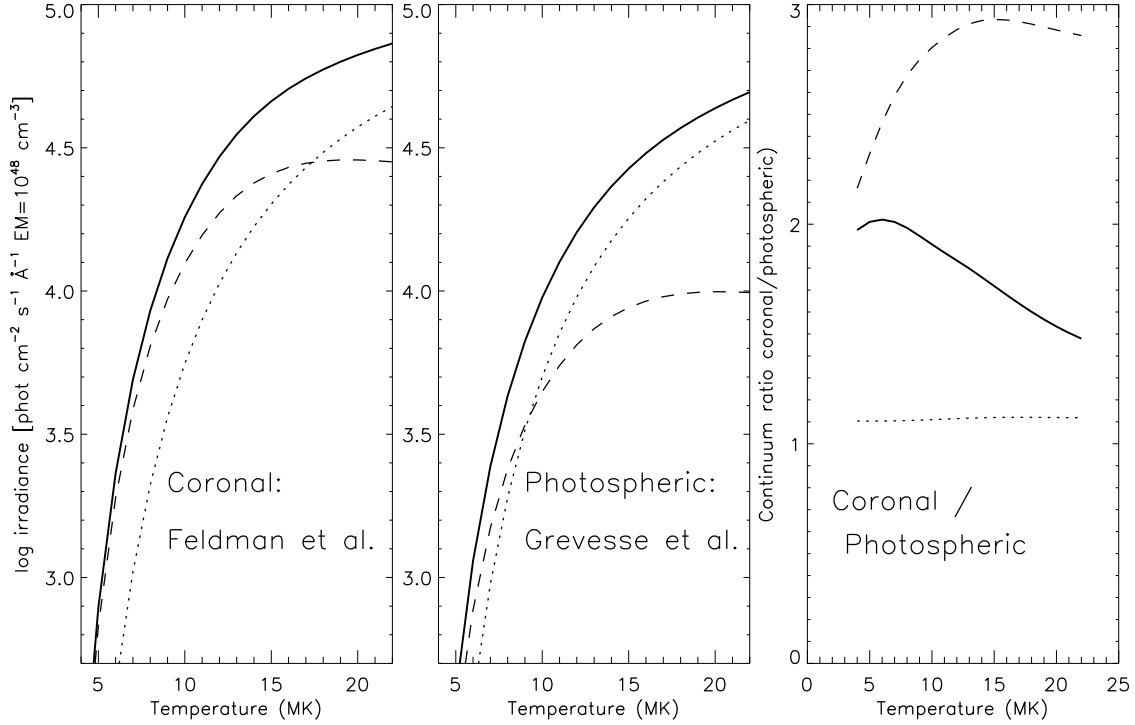


Fig. 2.— Continuum fluxes (irradiances, photon units) at 3.495 \AA as a function of T_e calculated from the CHIANTI atomic package. *Left panel:* Continua with the Feldman (1992) coronal abundances. *Center panel:* Continua with the Grevesse et al. (2007) photospheric abundances. *Right panel:* Ratio of continuum fluxes calculated with the Feldman (1992) abundances to those calculated with the Grevesse et al. (2007) abundances. The dashed curves refer to free-bound continua, dotted curves to free-free continua, and solid curves to the sum of all continua. Two-photon continua are not shown; they are a factor 30 or more lower than the free-free continuum.

(photons $\text{cm}^{-2} \text{s}^{-1} \text{\AA}^{-1}$) using calibration factors for both the crystal reflectivities and the proportional counter detectors; the procedure is described by Sylwester et al. (2005). The resulting fluxes are estimated to have a $\sim 20\%$ accuracy. RESIK was turned off during spacecraft passages through the South Atlantic Anomaly and the auroral ovals near the terrestrial poles (the spacecraft orbital inclination is 82.5°); at other times, there is a low particle background (between 0.01 and 0.05 counts $\text{bin}^{-1} \text{s}^{-1}$ for each of the four detectors, evaluated from observed counting rates in “hidden” or non-solar bins) which was subtracted from the observed counts in each detector.

The wavelengths chosen for estimating the continuum emission were centered on 3.495 \AA (width of range 0.051 \AA) and 3.762 \AA (0.028 \AA) for channel 1, and 3.840 \AA (0.051 \AA), 4.070 \AA (0.011 \AA), and 4.220 \AA (0.031 \AA) for channel 2. No significant line emission is known to occur in these ranges according to the CHIANTI atomic database and the spectral line list of Kelly (1987), though the S recombination edge at 3.846 \AA mentioned in §2 is within the third band. Fluxes in these wavelength ranges were determined for as many time intervals in flares as were available.

In our analysis, we assumed that a single temperature characterizes the emission in the 3.5–4.22 \AA range. This is not true for a wider wavelength range, but for spectroscopic purposes this is a good approximation for the narrow ranges considered here. To examine the temperature dependence of continuum fluxes, there are a number of options for finding the temperature. First, several line ratios are available, the most suitable being the ratios of Si XII dielectronic line features to Si XIII parent lines in channel 4 (Phillips et al. 2006a). However, these ratios are appropriate for softer wavelengths (up to 6 \AA) than those

¹The data are made available to the solar physics community via the World Wide Web site http://www.cbk.pan.wroc.pl/RESIK_Level2 based at the Space Research Centre, Wrocław, Poland.

Table 1. RESIK SPECTRA WITH CONTINUUM EMISSION

Date	Time of Flare Maximum (UT)	<i>GOES</i> Class	Location	Number of Spectra
2002 August 3	19:07	X1.0	S16W87	413
2002 September 10	14:56	M2.9	S10E43	235
2002 September 29	06:39	M2.6	N10E20	15
2002 October 4	05:38	M4.0	S19W09	317
2002 November 14	22:26	M1.0	S15E62	128
2002 December 4	22:49	M2.5	N14E63	12
2002 December 17	23:08	C6.1	S27E01	166
2003 January 7	23:30	M4.9	S11E89	113
2003 January 9	01:39	C9.8	S09W25	297
2003 January 21	02:28	C8.1	N14E09	69
2003 January 21	02:50	C4.0	N14E09	25
2003 January 21	15:26	M1.9	S07E90	290
2003 February 1	09:05	M1.2	S05E90	133
2003 February 6	02:11	C3.4	S16E55	34
2003 February 14	02:12	C5.4	N12W88	44
2003 February 14	05:26	C5.6	N11W85	64
2003 February 15	08:10	C4.5	S10W89	299
2003 February 22	04:50	B9.6	N16W02	19
2003 February 22	09:29	C5.8	N16W05	29

discussed here and are therefore likely to yield lower temperatures. Secondly, the ratio of total emission in RESIK channels 1 and 4, $I(3.40 - 3.80\text{\AA})/I(5.00 - 6.05\text{\AA})$, is sensitive to temperature ($T_{1/4}$) through the fact that the same Si lines as well as a Si XIV line are included in channel 4, while continuum and weak K XVIII lines are included in channel 1, with different temperature sensitivity. Thirdly, the ratio of the two *GOES* channels is a temperature indicator (T_{GOES}), this being widely used in previous analyses of flares. It was shown in previous work (Phillips et al. 2006a) that $T_{1/4}$ is linearly related to T_{GOES} . However, in the present analysis plots of the observed continuum flux against T_{GOES} were found to have significantly smaller scatter than those plotted against $T_{1/4}$, particularly when the emission in channel 1 was weak, suggesting that T_{GOES} is a better temperature indicator. We therefore chose to use T_{GOES} in the analysis of the RESIK spectra discussed here. The work of White et al. (2005) was used for the conversion of the *GOES* ratio to temperature T_{GOES} . In deriving T_{GOES} , we chose not to remove a pre-flare level from the *GOES* flux ratios since this was not done for the RESIK spectra. It is possible that estimates of T_{GOES} have lower precision for low ($T_{\text{GOES}} \lesssim 5$ MK) since for such temperatures the signal in the higher-energy *GOES* channel is relatively weak.

The plots of all continuum flux measurements against T_{GOES} are shown for the two continuum bands of channel 1 in Figure 3, together with the flux ratio of the two bands, and the three continuum bands of channel 2 in Figure 4. The logarithm of the flux is plotted, with the fluxes normalized to an emission measure of 10^{48} cm^{-3} . Each point represents an observed level of continuum in a time interval during the flares given in Table 1, with the temperature and emission measure estimated from the *GOES* ratio averaged over the time of each RESIK measurement. The total range of T_{GOES} is from 4 MK to 22 MK. The observed points are compared with calculated continua from the CHIANTI code with coronal abundances, shown as solid lines (abundance set of Feldman (1992)) and dashed lines (Fludra & Schmelz 1999), and photospheric abundances (Grevesse et al. 2007), shown

as dotted lines. The RESIK points agree significantly better with the CHIANTI curves assuming the Feldman (1992) coronal abundances for the continuum bands 3.495 Å and 3.762 Å, with the observed points occurring at higher fluxes than are predicted by the coronal abundances of Fludra & Schmelz (1999) or the photospheric abundances of Grevesse et al. (2007). The scatter of the points around the curve with the Feldman (1992) abundances is approximately 0.1 in the logarithm (26%). The standard deviation of the points is therefore less than this amount, in agreement with the estimated uncertainty in the RESIK absolute calibration ($\pm 20\%$). The observed ratios of these two bands (plotted in the right panel of Figure 3) are consistent with all three abundance sets. For the continuum fluxes in channel 2 (Figure 4), there is also agreement with the theoretical curves assuming the Feldman (1992) abundances to within measurement uncertainties for temperatures up to about 15 MK, above which the points are up to about 40% larger, slightly more than the estimated uncertainties. This departure may arise through the fact that a single temperature given by T_{GOES} less accurately describes the temperature of the emission: possibly a second component with different temperature is needed for these cases. Nearly all the observed points are above the other curves, by about 0.2 in the logarithm (60%) in the case of the Fludra & Schmelz (1999) abundance set and about 0.3 in the logarithm (a factor 2) in the case of the Grevesse et al. (2007) abundance set.

There are important implications for coronal element abundances in the curves of Figures 3 and 4. The agreement of the RESIK continuum fluxes with the CHIANTI curves with the Feldman (1992) abundances for the wavelength bands centered on 3.495 Å, 3.762 Å, 3.840 Å, 4.070 Å, and 4.220 Å implies that the abundances of elements giving rise to the largest contributions in these ranges, viz. Si, Fe, Mg, and O, are at least approximately correct. The Feldman (1992) abundances of Si, Fe, and Mg are approximately a factor 2 more than those of Fludra & Schmelz (1999), and the abundance of O 40% more. Thus, an abundance of Fe that is a factor 4 more than the photospheric (Grevesse et al. 2007)

is consistent with these results rather than one that is only a factor 2 more, as with the Fludra & Schmelz (1999) abundances. This is in agreement with Fe/H abundance results from an analysis of *RHESSI* thermal flare spectra (Phillips et al. 2006b). Out of 27 flares included in this analysis, 19 flares had an Fe/H abundance within 20% of the Feldman (1992) value; of the remaining eight flares, four had an Fe/H abundance more than 20% different from the Feldman (1992) value, while four flares had an equivocal result.

There are some points falling below all three theoretical curves, which are mostly those for the flare of 2003 February 22 (maximum time 09:29 U.T.). They are measured continuum fluxes for the initial stages of this flare, when it appears that an isothermal approximation for the emission is not a valid assumption as with other points in later stages of flares. Also, although there seems to be no significant departure from the curves for points in individual flares, indicating possible abundance variations during flares, we are investigating this in work in progress, in which line emission from particular elements is being used to evaluate abundances of some elements.

4. CONCLUSIONS

We have reported on measurements with the RESIK instrument of X-ray continuum emission at five line-free regions (3.495, 3.762, 3.840, 4.070, 4.220 Å) in a total of 2795 spectra in 19 solar flares. With temperature and emission measure determined from the ratio of emission in the two *GOES* channels, the RESIK continuum measurements, normalized to an emission measure of 10^{48} cm^{-3} , plotted against temperature of the observed emission closely follows the theoretical free-free and free-bound continuum using the CHIANTI atomic code with coronal abundances from Feldman (1992). The continuum measurements are about 60% higher than the curves for the Fludra & Schmelz (1999) abundances, and are higher by about a factor 2 than the summed free-free and free-bound

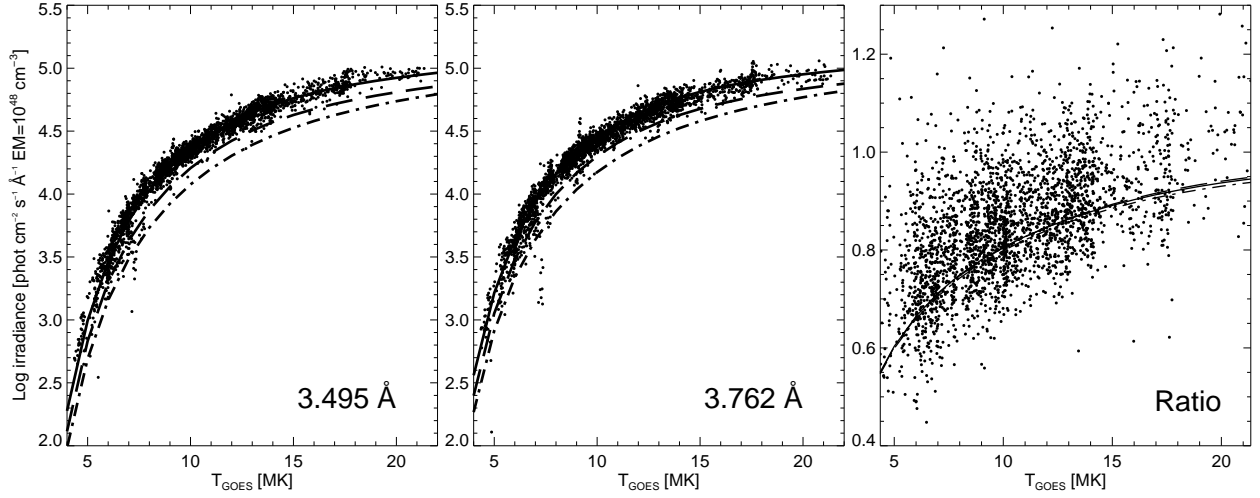


Fig. 3.— Measured continuum fluxes (points) in RESIK channel 1 at 3.495 Å (*left panel*) and 3.762 Å bands (*center*) plotted on a logarithmic scale against the temperature T_{GOES} determined from *GOES* ratios, all normalized to an emission measure of 10^{48} cm⁻³ (emission measure estimated from *GOES*). These are compared with calculated continua (free-free plus free-bound) from CHIANTI with the coronal abundances of Feldman (1992) (solid line), of Fludra & Schmelz (1999) (dashed line), and with the photospheric abundances of Grevesse et al. (2007) (dot-dash line). The ratio of the 3.495 Å and 3.762 Å continuum fluxes are shown in the right panel, with corresponding line styles.

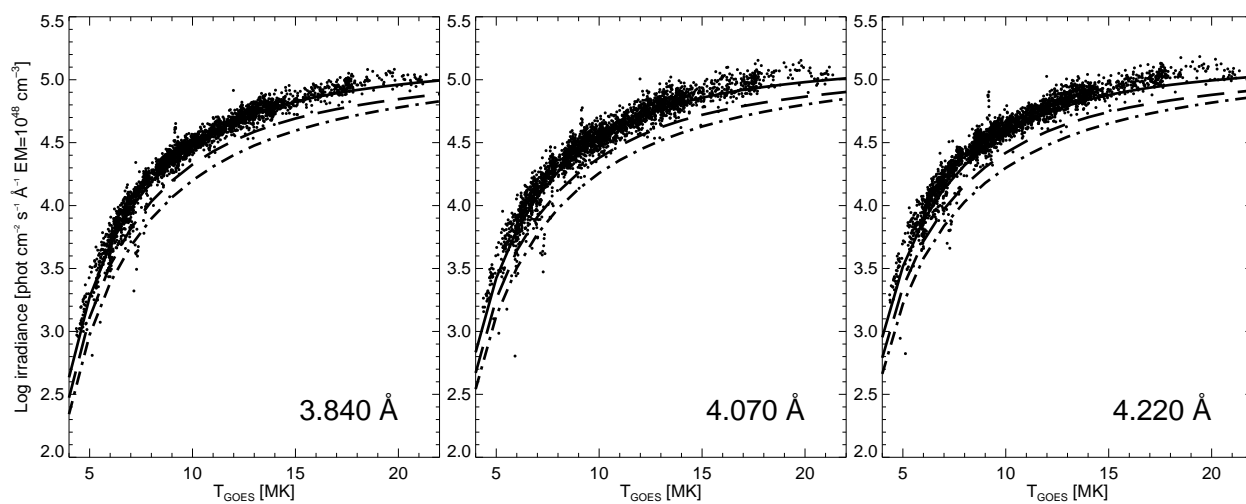


Fig. 4.— Measured continuum fluxes in RESIK channel 2 at 3.840 Å (*left panel*), 4.070 Å (*center*), and 4.220 Å bands (*right*) plotted on a logarithmic scale against T_{GOES} , normalized to an emission measure of 10^{48} cm^{-3} . Calculated continua with the coronal abundances of Feldman (1992) (solid line), Fludra & Schmelz (1999) (dashed line), and photospheric abundances of Grevesse et al. (2007) (dot–dash line).

continua calculated with the photospheric abundances of Grevesse et al. (2007). Thus the observed continuum in these spectral regions is consistent with the coronal abundances of Feldman (1992), suggesting that the abundances of those elements (O, Si, Mg, Fe) which are large contributors to the free-bound continuum are about four times photospheric for this sample of flares. Apart from points taken during the initial stages of the flare of 2003 February 22 (maximum 09:29 U.T.), an isothermal plasma assumed in this work appears to be justified in the narrow wavelength bands studied here. In work in progress, in which RESIK flare continua are compared with those at other wavelengths from *RHESSI*, the emitting plasma will be taken to have a multi-temperature structure.

We are grateful for financial help from the European Commission’s Seventh Framework Programme (FP7/2007-2013) under grant agreement No. 218816 (SOTERIA project, www.soteria-space.eu), the Polish Ministry of Education and Science Grant N N203 381736, and the UK–Royal Society/Polish Academy of Sciences International Joint Project (grant number 2006/R3) for travel support. CHIANTI is a collaborative project involving Naval Research Laboratory (USA), the Universities of Florence (Italy) and Cambridge (UK), and George Mason University (USA).

REFERENCES

- Asplund, M., Grevesse, N., Sauval, A. J., & Scott, P. 2009, *ARA&A*, 47, 481
- Brown, J. C., Mallik, P. C. V., & Badnell, N. R. 2009, *A&A*, in press (preprint arXiv:0912.3385v1)
- Bryans, P., Landi, E., & Savin, D. W. 2009, *ApJ*, 691, 1540
- Chifor, C., DelZanna, G., Mason, H. E., Sylwester, J., Sylwester, B., Phillips, K. J. H. 2007, *A&A*, 462, 323
- Culhane, J. L., & Acton, L. W. 1970, *MNRAS*, 151, 141
- Culhane, J. L., et al. 1991, *Sol. Phys.*, 136, 89
- Feldman, U. 1992, *Physica Scripta*, 46, 202
- Feldman, U., & Laming, J. M. 2000, *Physica Scripta*, 61, 222
- Fludra, A., & Schmelz, J. T. 1999, *A&A*, 348, 286
- Freeland, S. L., & Handy, B. N. 1998, *Sol. Phys.*, 182, 497
- Grevesse, N., Asplund, M., & Sauval, A. J. 2007, *Space Sci. Rev.*, 130, 105
- Gronenschild, E. H. B. M., & Mewe, R. 1978, *A&AS*, 32, 283
- Itoh, N., Sakamoto, T., Kusano, S., Nozawa, S., & Kohyama, Y. 2000, *ApJS*, 128, 1251
- Kelly, R. L. 1987, *Atomic and Ionic Spectrum Lines below 2000 Angstroms*, *J. Phys. Chem. Ref. Data*, 16, Supplement 1
- Landi, E., DelZanna, G., Young, P. R., Dere, K. P., Mason, H. E., & Landini, M. 2006, *ApJS*, 162, 261

Phillips, K. J. H., Dubau, J., Sylwester, J., Sylwester, B. 2006a, ApJ, 638, 1154

Phillips, K. J. H., Chifor, C., & Dennis, B. R. 2006b, ApJ, 647, 1480

Sutherland, R. S. 1998, MNRAS, 300, 321

Sylwester, B., Sylwester, J., & Phillips, K. J. H. 2009, A&A, submitted

Sylwester, J. et al. 2005, Sol. Phys., 226, 45

Sylwester, J., Sylwester, B., Landi, E., Phillips, K. J. H., & Kuznetsov, V. D. 2006, Adv.
Space Res., 36, 2871

Sylwester, J., Sylwester, B., & Phillips, K. J. H. 2008, ApJ, 681, L117

White, S. M., Thomas, R. J., & Schwartz, R. A. 2005, Sol. Phys., 227, 231